Research Article | Vol. 56, No. 25 / September 1 2017 / Applied Optics 7059

applied optics

Improved generation method utilizing a modified Fourier spectrum for Airy beams with the phase-only filter technique

JIANYONG LING,[1] QINGYUN YANG,[1] SHIXUE ZHANG,[1] QIANG LU,[1,2] SHUAI LIU,[1] AND CHENZI GUO[1,2,*]

[1]Changchun Institute of Optics, Fine Mechanics and Physics, Chinese Academy of Sciences, Dongnanhu Road 3888, Changchun 130033, China
[2]University of Chinese Academy of Sciences, Beijing 100049, China
*Corresponding author: guochenzi567@163.com

Received 22 May 2017; revised 28 July 2017; accepted 1 August 2017; posted 1 August 2017 (Doc. ID 296483); published 24 August 2017

We present an improved method to generate Airy beams utilizing a liquid crystal on silicon (LCoS) device. In this method, the phase and amplitude information of a modified Fourier spectrum of an Airy beam together with a Fresnel holographic lens is encoded onto the LCoS using the phase-only filter technique; thus, a desired Airy beam is formed in the focal plane of the Fresnel holographic lens. In this paper, the principle of the proposed method is described in detail, and both the excellent numerical simulations and experimental results for verifying this method are demonstrated. It is shown that the new generation method is accurate and simple; in particular, the setup is more compact compared to the conventional Fourier transform method, which comprises only the input polarized laser and a LCoS device. This effective method will further promote investigations into the properties and applications of Airy beams.

OCIS codes: (060.5060) Phase modulation; (050.1940) Diffraction; (090.1760) Computer holography; (070.7345) Wave propagation; (070.6120) Spatial light modulators.

https://doi.org/10.1364/AO.56.007059

1. INTRODUCTION

In 1979, Berry and Balazs found the Airy packets in the context of Quantum mechanics by solving the Schrödinger equation [1]. And the first experimental generation of Airy beams in a laboratory was proposed in 2007 by Siviloglou and Christodoulides [2,3]. From that moment, this unique type of beam has been an active area of research, including its generation methods, trajectory control, and practical applications. It is well known that an Airy beam, one of the no-diffraction beams, presents "self-healing" and "self-bending" features in propagation. These unusual properties give Airy beams a wide range of applications, such as vacuum electrons [4], optical trapping [5], microparticle clearing [6,7], surface plasmon polaritions [8], and free-space optical communication [9].

An accurate and efficient generation method for an Airy beam will contribute to deep research on the properties and propagation characteristics of Airy beams, which results in expanding its potential fields of practical applications. Several methods for generating an Airy beam with the help of different devices and materials have been reported, e.g., the approach using a continuous cubic phase plate [10], the method of Airy surface plasmons [11], generation by an engineered nanoscale phase grating [12], and the Airy beam laser [13,14]. The disadvantage of those approaches is that the profile and propagation trajectory of the generated Airy beam are invariable, so researchers cannot adjust the parameters of the Airy beam in experiments at any time.

To solve this problem, the phase information (a cubic phase) of the Fourier spectrum of the Airy beam is encoded onto the liquid crystal on silicon (LCoS) under phase-only modulation, and a Gaussian beam with an appropriate waist is used to illuminate the device to generate Airy beams in the image plane [2,3]. This is the conventional Fourier transform method (FTM). Due to utilization of the LCoS device, FTM presents the advantage of programmable adjustments. However, the optical Fourier transform system has a rather large length of $2f$, where the focal length f is as long as 1 m, usually. Moreover, the waist diameter of the Gaussian beam must be carefully prepared to match the phase loaded onto the LCoS.

As an improvement, the method to directly generate an Airy beam by encoding a 3/2 phase pattern onto the LCoS is proposed [15,16]. The advantage of this approach is not requiring the extensive system length used in the Fourier transform process. However, this method ignores the amplitude term $x^{3/2}$ for simplicity. Another method by combining the cubic phase and a Fresnel holographic lens together to generate an Airy beam is experimentally presented [17]. It reduces the distance between the LCoS device and the Fourier transform lens in FTM. In what we refer to as the Fresnel holographic lens method

1559-128X/17/257059-08 Journal © 2017 Optical Society of America

(FHLM), the shape of the generated Airy beam increases, and the deflection of it decreases, which indicates the generated quasi-Airy beam deviates the theoretical one. Although a Fresnel diffraction phase is used to compensate this problem, there is no quantitative analysis on the formed Airy beam in this reference. In addition, FHLM retains the preparation process of the Gaussian waist diameter. Recently, the quantitative properties of the generated Airy beam using FHLM together with the formula of the deflection of the main lobe are derived [18]. It is shown that the additional square phase term superimposing onto the Fourier transform result is the reason for the deterioration of FHLM.

In general, it has failed to generate an Airy beam directly using the LCoS device, because the phase and amplitude information of a complex cannot be arbitrarily modulated together accurately. As an indirect approach, FHLM successfully changes the optical system into a compact one, not only reducing half of the system length but also removing the physical lens. However, the additional square phase term in the result of FHLM is the main problem to overcome. If some approaches are adopted to counteract this square phase term, a meaningful method to generate an Airy beam can be demonstrated.

In this paper, we present an improved method for generating an Airy beam with a compact optical system, which comprises only the input light beam and a reflective LCoS device. The improved method works well and avoids the careful preparation of the Gaussian waist diameter. It is realized by utilizing the phase-only filter technique to encode the amplitude and phase information of a modified Fourier spectrum of an Airy beam and a Fresnel holographic lens onto the LCoS. The detailed principle description of the new method is demonstrated. After that, the corresponding numerical simulations of this method together with FTM and FHLM are illustrated. Finally, the experimental demonstration of generating Airy beams using the proposed method is presented.

2. PRINCIPLE DESCRIPTION

In this section, we briefly review the Airy beam and its Fourier spectrum theory and two conventional generation methods (FTM and FHLM). Then, the principle description of the improved method for generating Airy beams is described in detail.

A. Airy Beam and Its Fourier Spectrum

The finite-energy 2D Airy packet, which is a solution to the Helmholtz equation, can be expressed as

$$\begin{aligned}\phi(s_x, s_y, \xi) = \mathrm{Ai}\left[s_x - \left(\frac{\xi}{2}\right)^2 + ia\xi\right] \times \mathrm{Ai}\left[s_y - \left(\frac{\xi}{2}\right)^2 + ia\xi\right] \\ \times \exp\left(as_x - \frac{a\xi^2}{2} - \frac{i\xi^3}{12} + ia^2\frac{\xi}{2} + is_x\frac{\xi}{2}\right) \\ \times \exp\left(as_y - \frac{a\xi^2}{2} - \frac{i\xi^3}{12} + ia^2\frac{\xi}{2} + is_y\frac{\xi}{2}\right),\end{aligned} \quad (1)$$

where a is the decay factor, a small positive parameter associated with the effective aperture of the system; $s_x = x/x_0$ and $s_y = y/y_0$ are dimensionless transverse coordinates of the Airy packet; (x_0, y_0) is the arbitrary transverse scale; and $\xi = z/(kx_0^2)$ is a normalized propagation distance. At the origin $(z = 0)$, Eq. (1) can be rewritten as $\phi(s_x, s_y, \xi = 0) = \mathrm{Ai}(s_x)\exp(as_x)\mathrm{Ai}(s_y)\exp(as_y)$.

The Fourier transform of the finite-energy 2D Airy packets at the origin can be described as

$$\begin{aligned}\Phi(k_x, k_y) = \iint_{-\infty}^{+\infty} \phi(s_x, s_y, 0)\exp[2\pi i(s_x k_x + s_y k_y)]\mathrm{d}s_x\mathrm{d}s_y \\ \propto \exp[b(k_x^2 + k_y^2)]\exp\left[\frac{i(k_x^3 + k_y^3)}{3}\right],\end{aligned} \quad (2)$$

where b is a constant, and (k_x, k_y) are the spatial frequency coordinates in the Fourier spectrum space. According to Eq. (2), the spectrum of 2D Airy beam packets is Gaussian and involves of a cubic phase.

B. Two Conventional Generation Methods for Airy Beams

The Fourier transform method was first used by Siviloglou to experimentally generate finite-energy 1D and 2D Airy beams [2,3]. Figure 1(a) demonstrates the schematic of FTM. In this conventional method, a $2f$ optical system is employed to realize the optical Fourier transform. Two planes, defined as the phase plane and image plane, respectively, fit the Fourier transform relationship of each other. The cubic phase of the Fourier spectrum is imposed onto an input Gaussian beam in the phase plane, usually by a reflective LCoS providing the phase-only modulation. In this way, an Airy beam is formed in the image plane. It is noted that a physical lens with high quality is required in this method.

The Fourier transform between the image plane and the phase plane in FTM can be expressed as

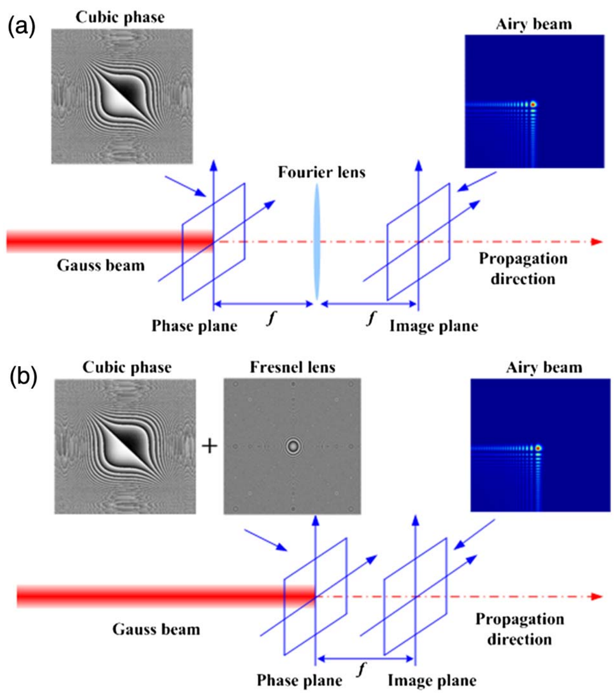

Fig. 1. Schematic of two conventional optical Fourier systems to generate an Airy beam. (a) FTM, (b) FHLM.

$$-i/\lambda f \iint_{-\infty}^{+\infty} \Phi(k_x, k_y) \exp[-2\pi i(s_x k_x + s_y k_y)] \mathrm{d}k_x \mathrm{d}k_y = -i/\lambda f \phi(s_x, s_y, 0). \quad (3)$$

The deflection of the main lobe of the generated Airy beam in x direction can be described as

$$x = \frac{z^2}{4\ k^2 x_0^3}. \quad (4)$$

The FHLM is proposed to reduce the large system length, in which a Fresnel holographic lens is utilized instead of a physical lens, and the distance between the Fresnel lens and the LCoS is reduced. The principle of this method can be interpreted by Fig. 1(b). The cubic phase of the Fourier spectrum and the Fresnel holographic lens is combined and directly loaded onto the input Gaussian beam in the phase plane. Ultimately, a quasi-Airy beam is obtained at the back focal plane of the Fresnel holographic lens (the image plane).

In FHLM, the relationship between the image plane and the phase plane based on the Huygens–Fresnel principle can be expressed as [17]

$$\begin{aligned}\phi'(s_x, s_y, 0) &= -\frac{i}{\lambda f} \iint_{-\infty}^{+\infty} \exp\left[-i\frac{\pi}{\lambda f}(k_x^2 + k_y^2)\right] \times \Phi(k_x, k_y) \\ &\quad \times \exp\left[\frac{\pi i}{\lambda f}[(s_x - k_x)^2 + (s_y - k_y)^2]\right] \mathrm{d}k_x \mathrm{d}k_y \\ &= -\frac{i}{\lambda f} \exp\left[i\frac{\pi}{\lambda f}(s_x^2 + s_y^2)\right] \phi(s_x, s_y, 0), \end{aligned} \quad (5)$$

where the Fourier transform is realized by the Fresnel holographic lens, described as $\varphi_F = \pi \times [x^2 + y^2]/\lambda f$ [19]. Here, f stands for focal length of the Fresnel holographic lens. From Eq. (5), we find that an additional square phase term $\exp[i\pi(s_x^2 + s_y^2)/\lambda f]$ is introduced into the Fourier transform result. It is a spherical aberration and will magnify the generated Airy beam relative to the ideal results.

The deflection of the main lobe of the quasi-Airy beam in x direction can be described as [18]

$$x = \frac{cz^2}{f + z}, \quad (6)$$

where c is a constant. Equation (6) shows that the propagation trajectory of the Airy beam generated using FHLM is no longer a parabola propagation trajectory.

C. Improved Method for Generating Airy Beams

Based on the FHLM, we modulate both the phase and amplitude information of a modified Fourier spectrum onto the input plane wave at the phase plane, in order to eliminate the additional square phase term of the Fourier transform result in the image plane. In this case, the properties of the generated Airy beam are entirely the same as the theoretical Airy beam. The schematic of the improved method to generate the Airy beam is demonstrated in Fig. 2 In this approach, the Fresnel lens is also employed to make the experimental setup compact, and to keep the mathematical transform relationship between the phase plane and the image plane invariable, expressed as Eq. (5).

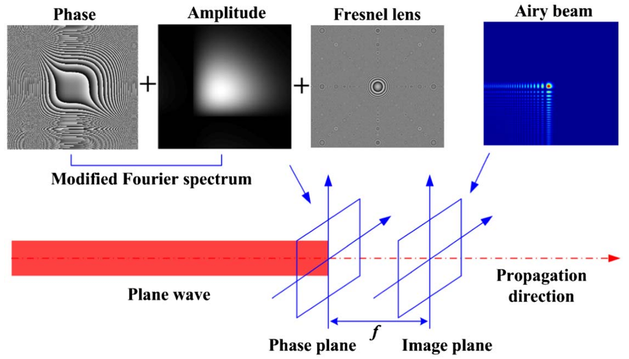

Fig. 2. Schematic of the improved method for generating an Airy beam.

The modified Fourier spectrum of the Airy beam used in the improved method loading onto the input plane wave at the phase plane is defined as

$$\Phi_1(k_x, k_y) = \iint_{-\infty}^{+\infty} \phi_1(s_x, s_y, 0) \exp[2\pi i(s_x k_x + s_y k_y)] \mathrm{d}s_x \mathrm{d}s_y = A(k_x, k_y) \exp(i\varphi(k_x, k_y)), \quad (7)$$

where

$$\phi_1(s_x, s_y, 0) = \exp\left[-i\frac{\pi}{\lambda f}(s_x^2 + s_y^2)\right] \phi(s_x, s_y, 0), \quad (8)$$

and $A(k_x, k_y) \exp(i\varphi(k_x, k_y))$ is the complex-value expression form of Eq. (7). According to Eq. (5), the Fourier transform result in the image plane is given by

$$\begin{aligned}\phi_1'(s_x, s_y, 0) &= -\frac{i}{\lambda f} \exp\left[i\frac{\pi}{\lambda f}(s_x^2 + s_y^2)\right] \\ &\quad \times \iint_{-\infty}^{+\infty} \Phi_1(k_x, k_y) \times \exp[-2\pi i(s_x k_x + s_y k_y)] \mathrm{d}k_x \mathrm{d}k_y,\end{aligned} \quad (9)$$

here, $\iint_{-\infty}^{+\infty} \Phi_1(k_x, k_y) \exp[-2\pi i(s_x k_x + s_y k_y)] \mathrm{d}k_x \mathrm{d}k_y$ stands for the Fourier transform of $\Phi_1(k_x, k_y)$. According to Eq. (7), $\phi_1(s_x, s_y, 0) = \iint_{-\infty}^{+\infty} \Phi_1(k_x, k_y) \exp[-2\pi i(s_x k_x + s_y k_y)] \mathrm{d}k_x \mathrm{d}k_y$. Thus, the final Fourier transform result in the image plane is given by

$$\begin{aligned}\phi_1'(s_x, s_y, 0) &= -\frac{i}{\lambda f} \exp\left[i\frac{\pi}{\lambda f}(s_x^2 + s_y^2)\right] \phi_1(s_x, s_y, 0) \\ &= -\frac{i}{\lambda f} \phi(s_x, s_y, 0) \exp\left[i\frac{\pi}{\lambda f}(s_x^2 + s_y^2) - i\frac{\pi}{\lambda f}(s_x^2 + s_y^2)\right] \\ &= -\frac{i}{\lambda f} \phi(s_x, s_y, 0).\end{aligned} \quad (10)$$

The generated Airy beam using the improved method has the identical expression as the conventional FTM, described by Eq. (1). The deflection function is also expressed as $x = z^2/4\ k^2 x_0^3$.

It is well known that the phase-only filter technique is capable of generating an arbitrary complex-valued function into the first diffraction order of the phase-only filter at the image plane. It is realized by encoding the phase and amplitude information of the Fourier spectrum for the complex-valued function onto the phase grating at the phase plane [17,20]. In our case, we take advantage of the phase-only filter to codify a complex-valued function, $A(k_x, k_y)\exp(i\varphi(k_x, k_y))$, onto a plane wave at the phase plane. The detailed process is illustrated as follows. First, a 45° oriented linear phase grating is designed in the phase plane, which can be expressed as

$$\varphi_p(k_x, k_y) = \frac{2\pi(k_x, k_y)}{d}, \tag{11}$$

where d is the period of the phase grating. Then, add the phase term $\varphi(k_x, k_y)$ and the linear grating together to come up with a result $\varphi_p(k_x, k_y) + \varphi(k_x, k_y)$, defined between the range $[-\pi, \pi]$. Following this, the amplitude information $A(k_x, k_y)$ is encoded by spatially modulating the phase filter, described as

$$\exp\{iA(k_x, k_y)[\varphi_p(k_x, k_y) + \varphi(k_x, k_y)]\}, \tag{12}$$

where $0 \le A(k_x, k_y) \le 1$, normalized by the maximum. Finally, a distorted modulation function $A'(k_x, k_y)$ is calculated by creating an appropriate lookup table for compensating the slight amplitude distortion caused by the sinc function [20]. The desired amplitude compensation function can be expressed as

$$\frac{\sin\{\pi[1 - A'(k_x, k_y)]\}}{\pi[1 - A'(k_x, k_y)]} = A(k_x, k_y), \tag{13}$$

where $0 \le A'(k_x, k_y) \le 1$. Therefore, the total phase loading onto the LCoS device in the phase plane can be written as

$$\exp\{iA'(k_x, k_y)[\varphi_p(k_x, k_y) + \varphi(k_x, k_y)]\}. \tag{14}$$

Through the Fourier transform, a complex-valued function, $A(k_x, k_y)\exp(i\varphi(k_x, k_y))$, is acquired in the first diffraction order in the image plane.

In this paper, we call the improved method with a phase-only filter "PFM" for short.

3. NUMERCIAL SIMULATION

In simulation, the multiple-phase screen method [21] is used to calculate the propagation dynamics of the generated Airy beam of the FTM, the FHLM, and the PFM, respectively. In particular, we focus on the intensity distributions and the deflections at different propagation distances of the generated Airy beams using these three methods.

The parameters for numerical calculation are taken as follows: the arbitrary transverse scale x_0, y_0 is 30 μm, the decay factor a is 0.03, the wavelength is 632.8 nm, the focal lengths of Fourier transform and the Fresnel holographic lens are 200 mm, the simulated size is 0.8 mm × 0.8 mm, the corresponding scale bar is 100 μm, and the propagation distance at the image plane is defined as 0 m. In FTM, the input beam is a Gaussian beam with the beam waist 50 mm at the phase plane. The cubic phase of the Fourier spectrum of the Airy beam is one screen at the phase plane, while the other screen is the physical lens behind the phase plane 200 mm, in which we use a 200 mm Fresnel holographic lens to replace it. In FHLM, there is only one screen at the phase plane, superposing the cubic phase of the Fourier transform and the Fresnel holographic lens together. And the input beam is also a Gaussian beam with the beam waist 50 mm at the phase plane. For PFM, the input beam is a 50 mm diameter plane wave, and the Fourier transform of Eq. (8) is modulated onto the input plane wave at the phase plane.

Figure 3 illustrates the simulated results of the three methods, in which Figs. 3(a1)–3(a3) stand for the intensity distributions of the FTM at 0 m, 0.025 m, and 0.035 m, respectively. Figures 3(b1)–3(b3) and 3(c1)–3(c3) correspond to the intensity distributions of the FHLM method and the PFM at the same distances (0 m, 0.025 m, and 0.035 m). As predicted, the generated Airy beams of the PFM are entirely the same as the FTM at different distances. It proves that the method we proposed to compensate the additional square phase aberration is correct and effective. However, the main lobes of the generated Airy beams using the FHLM are obviously bigger than the other two methods at distances 0.025 m and 0.035 m. The reason is the additional square phase term, which is caused by removing the distance f between the phase plane and the Fresnel holographic lens, resulting in the magnified intensity distributions. In addition, it is shown that the intensity distributions of the three methods at distance 0 m are the same as each other, which can be interpreted using Eqs. (3), (5), and (10). Under the calculation of the intensity value in Eq. (5), the additional square phase term is offset due to the multiplication of the complex conjugate at distance 0 m.

Figure 4 shows the normalized intensity values of the three methods at distances (a) 0 m, (b) 0.025 m, and (c) 0.035 m, respectively. The intensity value in every figure is normalized by the maximum of the method itself. There are some conclusions, as can be seen: first, the intensity distributions at distance 0 m of the three methods are coincident, as shown in Fig. 4(a),

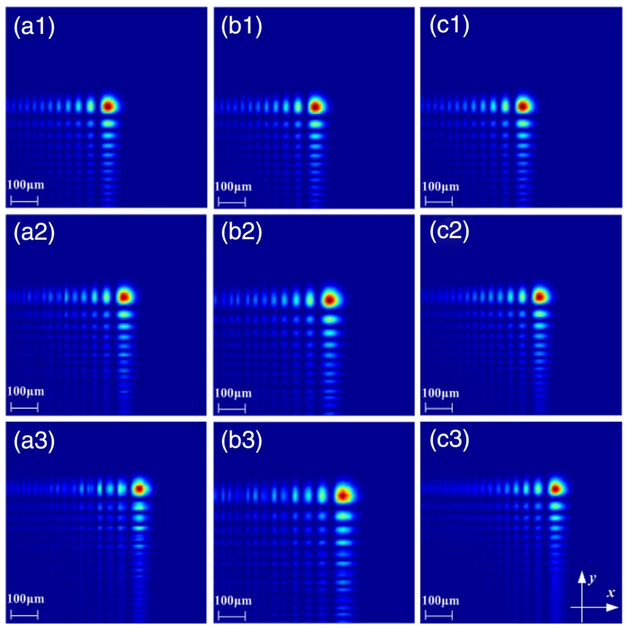

Fig. 3. Intensity distributions of the simulated Airy beams using three methods at different distances. (a1)–(a3) stand for the intensity distributions of the FTM at 0 m, 0.025 m, and 0.035 m, respectively, and (b1)–(b3) and (c1)–(c3) correspond to the intensity distributions of the FHLM and the PFM at the same propagation distances (0 m, 0.025 m, and 0.035 m).

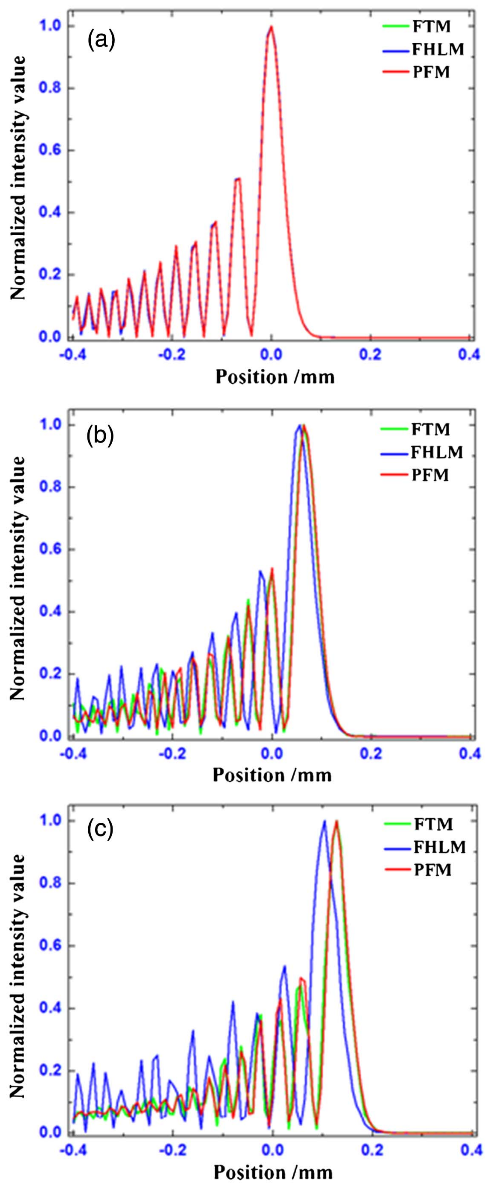

Fig. 4. Normalized intensity values along the vertical direction of the three methods at distances (a) 0 m, (b) 0.025 m, and (c) 0.035 m, respectively. The green, blue, and red lines stand for the FTM, the FHLM, and the phase-only filter method, respectively. The intensity values in every figure are normalized by the maximum of the method itself.

which we have explained above. Second, the normalized intensity values of the FTM and the PFM are basically coincident with each other at the three propagation distances. It declares the correctness of the PFM for compensating the square phase aberration. The slight difference in the intensity between them is caused by the beam waist diameter of the input Gaussian beam (50 mm) not absolutely matching the phase in FTM. Third, the full width at half maximum (FWHM) of the main lobes of the FTM and the PFM are 40 μm at distance 0 m and 48 μm at distance 0.035 m. However, the FWHM of the main lobe of the FHLM are 40 μm at distance 0 m and 64 μm at distance 0.035 m. It shows that after the same propagation

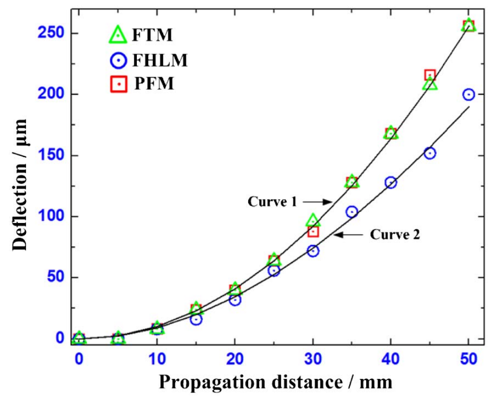

Fig. 5. Main lobes' deflections of the generated Airy beams using the three methods along x direction varying with the propagation distances, where the green triangle, blue circle, and red square correspond to the FTM, the FHLM and the PFM, respectively. Curve 1 stands for the fitting curve for the FTM and the PFM using Eq. (4), while curve 2 represents the fitting curve for the FHLM using Eq. (6).

distance, the diffraction of the FHLM is 1.33 times that of the FTM and the PFM. Finally, it is noted that the position of the main lobe of the FHLM obviously deviates the positions of the other methods (8 μm at distance 0.025 m and 24 μm at distance 0.035 m), because their deflection functions are different, as expressed by Eqs. (4) and (6).

To demonstrate the propagation trajectories of the generated Airy beams clearly, we draw the main lobes' deflections of the generated Airy beams of the three methods along x direction varying with the propagation distances, as shown in Fig. 5 The green triangle, blue circle, and red square correspond to the FTM, the FHLM, and the PFM, respectively. Through calculation, we find that the deflections of the FTM and the PFM are excellently described by curve 1, which fits Eq. (4) well, a parabola function. And the deflection of the FHLM, curve 2, fits Eq. (6) well. This phenomenon agrees with the theory we presented in Section 2.

4. EXPERIMENTAL GENERATION

In experiments, we present the formations of Airy beams using FTLM and PFM. The experimental setup, the detailed calculations of the phase masks, and the analysis of the experimental results for FTLM and PFM are illustrated, respectively. In order to compare FHLM and PFM, we use the same setup in the experiments. It indicates the input intensity and the beam waist is identical. In addition, the focal length of the Fresnel holographic lens and the size and position of the captured images are the same.

A. Setup

The schematic of the experimental setup is shown in Fig. 6, and the operation of the optical system can be described as follows. First, a HeNe laser (wavelength is 632.8 nm) goes through a beam expander to expand the Gaussian beam waist to 50 mm. Then, the expanded beam passes through a polarizer, which ensures the polarized direction of the incident beam parallel with the long axis of the liquid crystal molecules. After that,

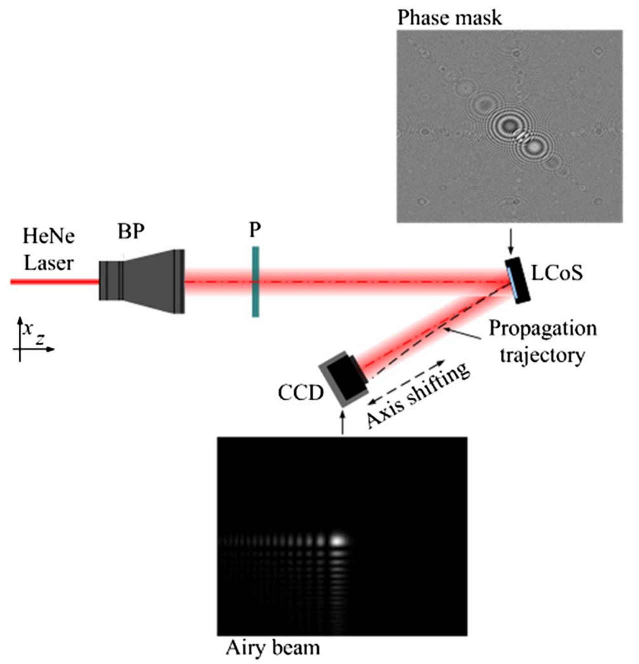

Fig. 6. Schematic of the experimental setup to generate Airy beams. HeNe laser is a collimated 632.8 nm laser, BP is the beam expander, P is a polarizer, LCoS is a refractive liquid crystal on silicon device, the black dotted line denotes the propagation trajectory of the generated Airy beam, and the black dotted arrow represents the axially scanning direction of the CCD camera.

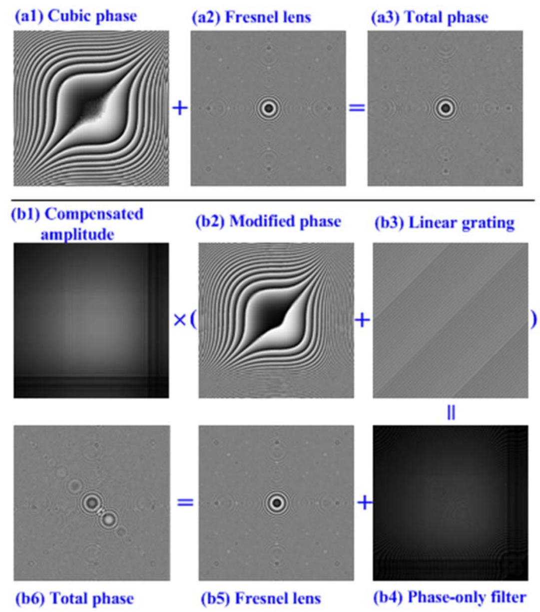

Fig. 7. Illustration of the phase mask for generating an Airy beam using FHLM and PFM. (a1) Cubic phase mask of the Fourier spectrum of an Airy beam, (a2) phase mask of a 170 mm Fresnel holographic lens, and (a3) total phase mask, which consists of (a1) and (a2). Compensated amplitude (b1) and phase (b2) of a modified Fourier spectrum of an Airy beam, (b3) 45° oriented linear grating, whose phase range is from -40π to 40π, (b4) phase-only filter computed by Eq. (14), (b5) phase mask of a 170 mm Fresnel holographic lens, (b6) total phase mask consisting of the Fresnel lens and the phase-only filter. Blank stands for grayscale value 0, white stands for grayscale value 255, and (0, 255) corresponds to $(0, 2\pi)$.

the beam gets to the LCoS device [22,23], of which the incident angle is about 5°. In phase-only modulation mode, the incident beam is modulated by loading a phase mask of an Airy beam onto the LCoS device. Finally, the propagation dynamics of a 2D Airy beam can be captured by a CCD camera, which can axially scan near the focal plane of the Fresnel lens.

The LCoS used in the experiment is a reflective device, which is manufactured by Holoeye incorporation. The device panel has 1920 × 1080 pixels in a 15.36 mm × 8.64 mm array, with a pixel pitch of 8 μm × 8 μm and 87% fill factor. The size of the captured image is 2 mm × 2 mm, and the corresponding scale bar in it is 250 μm.

B. Calculation of Phase Masks

The parameters for calculation of the phase masks [24] in the experiment are taken as follows: the arbitrary transverse scale x_0, y_0 is 26 μm, the decay factor a is 0.03, the wavelength is 632.8 nm, the focal lengths of Fourier transform and the Fresnel holographic lens are 170 mm, the phase range of the linear grating is from -40π to 40π, the size of the phase mask is 8.64 mm × 8.64 mm, the phase masks are sampled 1080 × 1080 pixels, and modulated in the range $[0, 2\pi]$.

Figure 7 illustrates the calculated phase mask for generating Airy beams using FHLM and PFM. For FHLM, first a cubic phase is obtained by extracting the phase information of the Fourier spectrum of the Airy beam, as shown in Fig. 7(a1). Second, a 170 mm Fresnel holographic lens is computed, as shown in Fig. 7(a2). Finally, the total phase mask is acquired by superposing the cubic phase and the Fresnel lens, as shown in Fig. 7(a3).

For PFM, the calculation process can be expressed as follows: 1) The compensated amplitude is computed according to Eq. (13), as shown in Fig. 7(b1). 2) The phase of a modified Fourier spectrum of the Airy beam is computed according to Eqs. (7) and (8), as shown in Fig. 7(b2). 3) The phase-only filter is obtained by combining the 45° oriented linear grating and the modified phase and then multiplying with the compensated amplitude, as shown in Fig. 7(b4). 4) The total phase mask is acquired by superposing the phase-only filter and a 170 mm Fresnel lens, as shown in Fig. 7(b6). The final phase mask for PFM [Fig. 7(b6)] uses a modified Fourier spectrum to compensate the additional square phase term, and adopts the phase-only filter technique to realize the phase and amplitude modulation together.

C. Experimental Results

Three intensity patterns of the generated Airy beams using FHLM and PFM at three distances (0.17 m, 0.18 m, and 0.19 m) after the LCoS device, corresponding to Figs. 8(a1, b1), 8(a2, b2), and 8(a3, b3), respectively, are captured in the experiment. Figures 8(a1)–8(a3) represent the captured figures of PFM, while Figs. 8(b1)–8(b3) denote the captured figures of FHLM. Several excellent conclusions from the experimental results in Fig. 8 are observed. First, the intensity profiles at the origin (170 mm), as seen in Figs. 8(a1) and 8(b1), are uniform basically, which agrees with the conclusion in simulation.

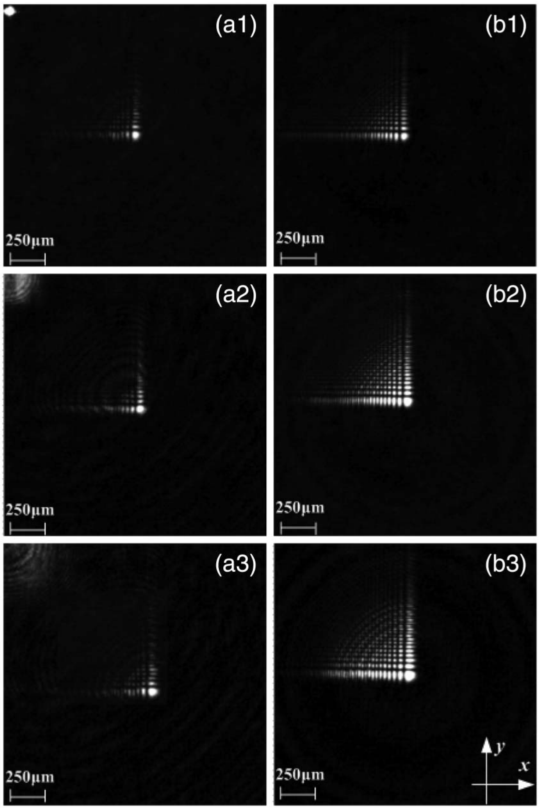

Fig. 8. Intensity distributions of the formed Airy beams using PFM and FHLM in the experiments. (a1)–(a3) represent the captured figures of PFM, while (b1)–(b3) denote the captured figures of FHLM, and (a1), (b1), (a2), (b2), and (a3), (b3) correspond to the intensity patterns after the LCoS 0.17 m, 0.18 m, and 0.19 m, respectively. The corresponding scale bar is 250 μm.

However, the brightness of the two figures is different, because the FHLM has no zero diffraction order, but the pattern of the PFM is in the first order, as we clearly see the zero diffraction order in the top left corner in Fig. 8(a1). Second, the propagation trajectories of the two methods are different, because the deflections of the generated Airy beams at the same distances are different, as shown in Figs. 8(a2, b2) and 8(a3, b3). Third, with the propagation increasing, the main lobes of FHLM are obviously bigger than the main lobes of PFM, as seen in Figs. 8(a2, b2) and 8(a3, b3). It indicates the diffraction in FHLM is stronger than in PFM.

Figure 9 demonstrates the normalized intensity profiles of the experimental results along x direction using PFM and FHLM at distances 0.17 m, 0.18 m, and 0.19m, respectively. Figures 9(a1)–9(a3) stand for PFM, while Figs. 9(b1)–9(b3) stand for FHLM. From Figs. 9(a1)–9(a3), the measurement FWHMs of the main lobes are about 50 μm, 56 μm, and 61 μm, respectively. And in Figs. 9(b1)–9(b3), the FWHMs of the main lobes are about 50 μm, 77 μm, and 94 μm, respectively. Namely, the diffraction of FHLM is 1.55 times that of PFM. It proves the derived result in Eq. (5), that the square spherical aberration magnifies the shapes of the generated Airy beams in FHLM.

The transverse accelerations in the x axis of the main lobes varying with propagation distances in PFM and FHLM are presented in Fig. 10 The red square represents the measurement results of PFM, and the blue circle represents the measurement results of FHLM. Curve 1 depicts a parabolic trajectory, which is well described by Eq. (4), while curve 2 indicates a fitting curve, as expressed by Eq. (6). Obviously, the deflection trajectory of PFM is closer to parabolic; however,

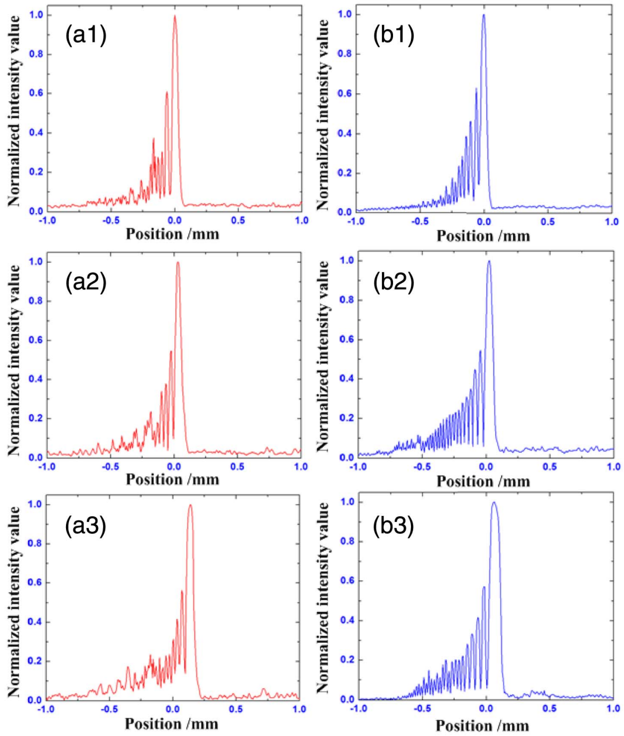

Fig. 9. Comparison of the normalized intensity profiles of PFM and FHLM along x direction at distances 0.17 m, 0.18 m, and 0.19m, respectively. (a1)–(a3) stand for PFM, while (b1)–(b3) stand for FHLM. The intensity value in every figure is normalized by the maximum of the method itself.

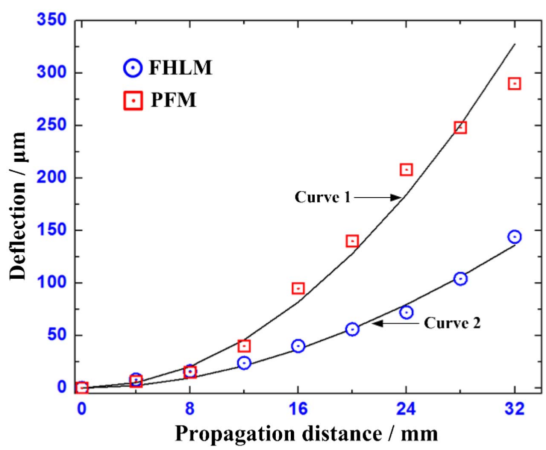

Fig. 10. Transverse accelerations in x axis of the main lobes along the propagation distances in PFM and FHLM. Red squares and blue circles represent the calculation results corresponding to PFM and FHLM. Curve 1 and curve 2 are the fitting lines according to Eqs. (4) and (6), respectively.

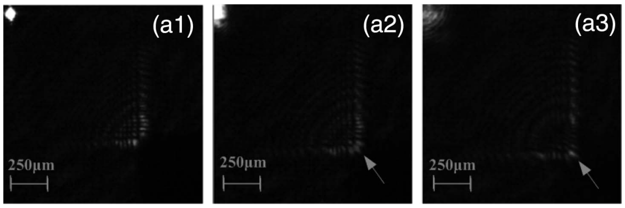

Fig. 11. Self-healing of the generated Airy beams using PFM with the main lobe obstructed at a distance of 0.17 m. (a1)–(a3) Corresponding intensity pattern after LCoS device at 0.17 m, 0.175 m, and 0.185m, respectively. The corresponding scale bar is 250 μm.

the deflection trajectory of FHLM is closer to the fitting line expressed by Eq. (6). This phenomenon has been explained by the theoretical relation presented in Section 2.

To demonstrate the self-healing properties of the generated Airy beams using PFM, we block the main lobe at distance 0.17 m, as seen in Fig. 11(a1). Also, we capture three intensity patterns at three distances, 0.170 m, 0.175 m, and 0.185 m, after the LCoS device, corresponding to Figs. 11(a1)–11(a3), respectively. It depicts the reformation of the main lobe beginning from a 5 mm propagation at distance 0.175 m, and the main lobe is reborn at the corner, clearly at distance 185 mm, which is marked using white arrows, as shown in Figs. 11(a2) and 11(a3).

In comparison, the formed Airy beams in PFM demonstrate the quasi-non-diffraction, the parabolic trajectory, and the self-healing property. It declares that the generated beam is the theoretical finite-energy Airy beam. However, the diffraction of the formed Airy beams in FHLM is more intense than PFM, and the propagation trajectory is not parabolic. It shows that the generated beam of FHLM is a quasi-Airy beam, not a theoretical finite-energy Airy beam.

5. CONCLUSIONS

An accurate method to experimentally generate an Airy beam is presented in this paper. It is realized by using a phase-only filter to encode the phase and amplitude information of a modified Fourier spectrum of an Airy beam onto the LCoS device, and through the Fourier transformation of the superimposed Fresnel holographic lens to generate an Airy beam at the image plane. Excellent numerical simulations and experimental results to verify the proposed approach are demonstrated. It shows that the formed beam is a theoretical finite-energy Airy beam compared to the quasi-Airy beam in FHLM. Meanwhile, the proposed method greatly simplifies the experimental setup and avoids the careful preparation process of the Gaussian beam waist by using an input plane wave. The meaningful method is useful to deeply investigate Airy beam in laboratory. In addition, the zero order diffraction in the generated result can be removed by directly being blocked or using a spatial filter system. And the improvement of the intensity of the generated Airy beam in the first order is worth devoting more attention to in research.

Funding. National High Technology Research and Development Program of China (2015AA0330).

REFERENCES

1. M. V. Berry and N. L. Balazs, "Nonspreading wave packets," Am. J. Phys. **47**, 264–267 (1979).
2. G. A. Siviloglou and D. N. Christodoulides, "Accelerating finite energy Airy beams," Opt. Lett. **32**, 979–981 (2007).
3. G. A. Siviloglou and D. N. Christodoulides, "Observation of accelerating Airy beam," Phys. Rev. Lett. **99**, 213901 (2007).
4. J. Li, X. Fan, W. Zang, and J. Tian, "Vacuum electron acceleration driven by two crossed Airy beams," Opt. Lett. **36**, 648–650 (2011).
5. Z. Zheng, B. Zhang, H. Chen, J. Ding, and H. Wang, "Optical trapping with focused Airy beam," Appl. Opt. **50**, 43–49 (2011).
6. J. Baumgartl, M. Mazilu, and K. Dholakia, "Optically mediated particle clearing using Airy wavepackets," Nat. Photonics **2**, 675–678 (2008).
7. A. M. Rubenchik, M. P. Fedoruk, and S. K. Turitsyn, "The effect of self-focusing on laser space-debris cleaning," Light Sci. Appl. **3**, e159 (2014).
8. S. S. Kou, G. Yuan, Q. Wang, L. Du, E. Balaur, D. Zhang, D. Tang, B. Abbey, X. Yuan, and J. Lin, "On-chip photonic Fourier transform with surface plasmon polaritons," Light Sci. Appl. **5**, e16034 (2016).
9. X. Chu, "Evolution of an Airy beam in turbulence," Opt. Lett. **36**, 2701–2703 (2011).
10. R. Cao, Y. Yang, and J. Wang, "Microfabricated continuous cubic phase plate induced Airy beams for optical manipulation with high power efficiency," Appl. Phys. Lett. **99**, 261106 (2011).
11. A. Salandrino and D. N. Christodoulides, "Airy plasmon: a nondiffracting surface wave," Opt. Lett. **35**, 2082–2084 (2010).
12. A. Minovich, A. E. Klein, and N. Janunts, "Generation and near-field imaging of Airy surface plasmons," Phys. Rev. Lett **107**, 116802 (2011).
13. S. Longhi, "Airy beams from a microchip laser," Opt. Lett. **36**, 716–718 (2011).
14. G. Porat, I. Dolev, and O. Barlev, "Airy beam laser," Opt. Lett. **36**, 4119–4121 (2011).
15. D. M. Cottrell, J. A. Davis, and T. M. Hazard, "Direct generation of accelerating Airy beams using a 3/2 phase-only pattern," Opt. Lett. **34**, 2634–2636 (2009).
16. J. A. Davis, D. M. Cottrell, and J. M. Zinn, "Direct generation of abruptly focusing vortex beams using a 3/2 radial phase-only pattern," Opt. Lett. **52**, 1888–1891 (2013).
17. J. A. Davis, M. J. Mitry, and M. A. Bandres, "Generation of accelerating Airy and accelerating parabolic beams using phase-only patterns," Appl. Opt. **48**, 3170–3176 (2009).
18. T. Latychevskaia, D. Schachtler, and H. W. Fink, "Creating Airy beams employing a transmissive spatial light modulator," Appl. Opt. **55**, 6095–6101 (2016).
19. B. Ma, B. Yao, Z. Li, M. Lei, S. Yan, P. Gao, D. Dan, and T. Ye, "Generation of three-dimensional optical structures by dynamic holograms displayed on a twisted nematic liquid crystal display," Appl. Phys. B **110**, 531–537 (2013).
20. J. A. Davis, D. M. Cottrell, J. Campo, M. J. Yzuel, and I. Moreno, "Encoding amplitude information onto phase-only filters," Appl. Opt. **38**, 5004–5013 (1999).
21. Y. Gu and G. Gbur, "Scintillation of Airy beam arrays in atmospheric turbulence," Opt. Lett. **35**, 3456–3458 (2010).
22. Z. Zhang, Z. You, and D. Chu, "Fundamentals of phase-only liquid crystal on silicon (LCOS) devices," Light Sci. Appl. **3**, e213 (2014).
23. W. Zhang, H. Zappe, and A. Seifert, "Wafer-scale fabricated thermo-pneumatically tunable microlenses," Light Sci. Appl. **3**, e145 (2014).
24. V. Bianco, P. Memmolo, M. Paturzo, A. Finizio, B. Jacidi, and P. Ferraro, "Quasi noise-free digital holography," Light Sci. Appl. **5**, e16142 (2016).